Localized Epigenetic Changes Induced by DH Recombination Restricts Recombinase to DJH Junctions

Published in final edited form as:
Nat Immunol. 2012 December ; 13(12): 1205–1212. doi:10.1038/ni.2447.

Localized Epigenetic Changes Induced by D_H Recombination Restricts Recombinase to DJ_H Junctions

Ramesh Subrahmanyam, **Hansen Du**, and **Irina Ivanova**
Laboratory of Molecular Biology and Immunology National Institute on Aging National Institutes of Health 251 Bayview Boulevard Baltimore, MD 21224

Tirtha Chakraborty[4], **Yanhong Ji**[1,2], **Yu Zhang**[3], **Frederick W. Alt**[3], and **David G. Schatz**[1]
Ranjan Sen
Laboratory of Molecular Biology and Immunology National Institute on Aging National Institutes of Health 251 Bayview Boulevard Baltimore, MD 21224

[1]Howard Hughes Medical Institute, Department of Immunobiology, Yale Medical School, 300 Cedar Street, Box 208011, New Haven, CT 06520-8011

[3]Howard Hughes Medical Institute, The Children's Hospital, Immune Disease Institute and Department of Genetics, Harvard Medical School, Boston, MA 02115

Abstract

Immunoglobulin heavy chain (*Igh*) genes are assembled by sequential rearrangements of diversity (D_H) and variable (V_H) gene segments. Three critical constraints govern V_H recombination. These include timing (V_H recombination follows D_H recombination), precision (V_Hs recombine only to DJ_H junctions) and allele specificity (V_H recombination is restricted to DJ_H recombined alleles). We provide a model for these universal features of V_H recombination. Analyses of DJ_H recombined alleles revealed that DJ_H junctions were selectively epigenetically marked, became nuclease sensitive and bound RAG proteins, thereby permitting D_H-associated recombination signal sequences to initiate the second step of *Igh* gene assembly. We propose that V_H recombination is precise because these changes did not extend to germline D_H gene segments located 5′ of the DJ_H junction.

INTRODUCTION

Genes that encode antigen receptors of lymphocytes are assembled via DNA recombination events that juxtapose gene segments spread over several megabases of the genome. V(D)J recombination, as this process is known, is precisely coordinated to the lineage- and developmental stage of lymphocytes[1,2]. Thus, immunoglobulin (Ig) genes rearrange in the B lymphocyte lineage whereas T cell receptor genes rearrange in the T lymphocyte lineage. Within the B lineage, Ig heavy chain (*Igh*) genes rearrange first, followed by Ig light chain (*Igk*, *Igl*) genes; similarly, within the T lineage *Tcrb* chain genes rearrange first followed by

Correspondence should be addressed to R.Se. (Senranja@grc.nia.nih.gov).
[2]Current address: Department of Immunology & Microbiology, School of Medicine, Xian Jiaotong University, 28 Xian ning West Road, Xian Shaanxi, China 710049
[4]Current address: ModeRNA Therapeutics, 161 First Street, Cambridge, MA 02142
AUTHOR CONTRIBUTIONS R.Su designed and performed all the experiments; R.Su. and R.Se. analyzed and interpreted the data; H.D. assisted with Southern blots; I.I. performed the H3K4me2 ChIP; T.C. assisted in the initial characterization of DJ_H-rearranged cell lines; Y.J. and D.G.S. provided D345 cells and ongoing discussion regarding RAG ChIP; Y.Z. and F.W.A. generated the E_μ-deficient cell lines; R.Su. and R.Se. wrote the manuscript; D.G.S. and F.W.A. read and critiqued the manuscript.

COMPETING FINANCIAL INTERESTS The authors declare no competing financial interests.

Tcra genes. The loci that rearrange first in each lineage (*Igh* and *Tcrb*) consist of variable (V), diversity (D) and joining (J) gene segments and require two recombination events to generate fully recombined alleles. In each case, D to J recombination precedes V recombination to the pre-formed DJ junction to produce VDJ recombined alleles. Thus, understanding antigen receptor gene assembly involves uncovering mechanisms that (a) select a locus for rearrangement and (b) impose the order of V(D)J recombination at the *Igh* and *Tcrb* loci.

V(D)J recombination requires recruitment of the recombination activating gene products, RAG1 and RAG2, to loci destined for rearrangement. Thereafter, RAG1-RAG2 introduce double-strand breaks at special recombination signal sequences (RSSs) that flank gene segments to initiate recombination. The accessibility of a locus to RAG recombinase determines the choice of the antigen receptor gene that will recombine. This is termed the accessibility hypothesis[3]. Accessibility, in turn, is regulated by *cis*-acting accessibility control elements (ACEs) which coincide with promoters and enhancers within antigen receptor loci[4]. At one level, therefore, the order of B cell antigen receptor gene rearrangements can be viewed as *Igh* accessibility preceding *Igk* accessibility, and within the *Igh* locus, D_H gene segments becoming accessible before the V_H gene segments.

From the earliest formulation of the accessibility hypothesis chromatin structure has been considered to be a key determinant of locus accessibility[5,6]; however, molecular features that distinguish between accessible and inaccessible loci are just beginning to be understood[7–9]. All antigen receptor loci contain acetylated histones prior to initiation of recombination in the appropriate lymphocyte lineage and at the appropriate developmental stage[1,4,10]. Where examined, rearrangeable loci are also marked with activation-associated histone methylation, such as di- or tri- methylation of lysine 4 of histone H3 (H3K4me2, me3). Conversely, the repressive histone modification H3 lysine 9 di-methylation (H3K9me2) is reduced prior to recombination[11,12]. Moreover, recruitment of the H3K9 methyl transferase G9a to recombination substrate attenuates recombination thereby providing direct evidence of the inhibitory effects of this modification[13]. The function of specific positive modifications in V(D)J recombination remains unclear, however, because it is difficult to modulate these marks independently of one another and assess the effects on recombination. The recognition that PHD domain of RAG2 binds H3K4me3 leads to a model where epigenetic histone modifications mark a locus for RAG1-RAG2 recruitment[14–16].

The *Igh* locus comprises approximately 150 V_H gene segments, 8–12 D_H gene segments and 4 J_H gene segments[17]. The initial activation of D_H (rather than V_H) recombination and the preferential usage of certain D_H gene segments are explained by several observations. First, analyses of RAG-deficient pro-B cells show that only the 5′-and 3′-most D_H gene segments (DFL16.1 and DQ52 respectively) and the region encompassing the J_H gene segments extending until the C_μ exons have hallmarks of active chromatin[11,18]. These include the presence of activating histone modifications, nuclease sensitivity and pockets of DNA demethylation (R. Selimyan, I.I, R.Su., F.W.A., R.Se, et al., submitted for publication). The absence of such marks at the V_H locus leads to a model that V_H gene segments are relatively inaccessible to recombinase at this stage[19]. Second, the J_H region exhibits the greatest density of RAG proteins within the *Igh* locus[20]; in contrast, RAG proteins are undetectable at V_H genes in pro-B cells. Thus, recombinase is perfectly positioned to initiate D_H rather than V_H recombination. Third, the 3′ end of the *Igh* locus has been proposed to fold into a 3-loop structure that places the 5′- and 3′-most D_H gene segments closest to the RAG-rich recombination center[21]. This spatial configuration maximizes the chance of J_H-associated RAG proteins to find complementary D_H-RSSs in the first recombination step. Fourth, a recombination barrier element has been recently identified 5′ of DFL16.1 that prevents V_H

recombination to germline D_H gene segments[22]. Binding sites for the insulator protein CTCF within this element are essential for barrier activity[23].

With plausible models for the regulation of D_H recombination in place, it is imperative to study the second step of *Igh* gene assembly. V_H recombination is regulated at multiple levels, such as preferential recombination of proximal V_H gene families, IL-7 responsiveness of the V_HJ558 genes located at the 5′ end of the locus, and feedback inhibition of V_H recombination[24,25]. Before these features of V_H gene segment selectivity come into play, however, three general aspects of V_H recombination must be addressed. First, why does V_H recombination always follow D_H recombination? Second, why does V_H recombination occur selectively on DJ_H recombined alleles? Third, what is the mechanism that directs V_H gene segments to recombine to the DJ_H junction? The exquisite precision of this latter point is noteworthy because the closest unrearranged D_H gene segment 5′ of a DJ_H junction is located only 4 kb away; yet, V_H gene segments from more than a megabase away find the DJ_H junction and not the adjacent germline D_H gene segment.

We reasoned that answers to these questions likely lay in the chromatin structure and RAG recruitment profile of DJ_H recombined alleles, and therefore analyzed changes that occur after the first step of *Igh* recombination. We demonstrate that DJ_H junctions were selectively activated as measured by highly localized changes in histone modifications and nuclease sensitivity. The absence of activating histone modifications on E_μ-deficient DJ_H recombined alleles points to a key role for E_μ in mediating these changes and explains the loss of V_H to DJ_H recombination on E_μ-deleted alleles. We also show that RAG1-RAG2 binding is re-distributed towards the DJ_H junction on WT alleles and does not extend to the closest unrearranged D_H gene segment. We propose D_H recombination brings the associated D_H-RSS to the recombination center, thereby permitting its use to initiate the second step of *Igh* gene assembly. Because RAG proteins are not present at upstream germline D_H gene segments to initiate recombination, V_H genes recombine specifically to the DJ_H junctions.

RESULTS

Localized activation of DJ_H junctions

To analyze the state of DJ_H rearranged loci we generated a panel of cell lines that contain specific *Igh* rearrangements. For this we transiently transfected RAG2-deficient fetal liver-derived 6312 cells with a RAG2 expression vector and isolated single-cell clones with recombined *Igh* alleles. Because RAG2 was expressed transiently these clones were genetically stable thereafter. D_H recombination was assayed by PCR (Supplementary Fig. 1) and we used representative clones in chromatin assays. We first examined the changes that accompany rearrangement of a DSP gene segment located in the middle of the D_H cluster. One allele in 2B9 cells has a DSP2.2b-J_H1 rearrangement and the second allele has undergone V_H recombination, thereby deleting all unrearranged D_H gene segments (Fig. 1a). We designed primers specific to the 5′ region of the rearranged DSP2.2b gene segment and compared the histone modification state of the DJ_H rearranged allele to germline alleles in the parental cell line.

Chromatin immunoprecipitation (ChIP) assays revealed that activation-related H3K9ac and K3K4me2 modifications were increased in the 3 kb region 5′ of the DJ_H junction (Fig. 1b, pink bars) compared to germline alleles (maroon bars). The γ-actin promoter and $C_\gamma3$ constant region served as positive and negative controls, respectively. Sequences close to the DJ_H junction were also depleted of suppressive H3K9me2 modifications and enriched in transcription-associated H3K4me3 (Fig. 1b). Abundance of H3K9me2 modification increased whereas H3K4me3 modification decreased, 3 kb 5′ of the DJ_H junction. These changes provided plausible explanations for our earlier analyses of DJ_H transcription. In

those studies we showed that DFL16.1 and DSP rearrangements activated promoters that were dormant in the germline configuration, resulting in increased RNA polymerase II (Pol II) recruitment and elevated sense- and anti-sense-oriented transcription from the DJ_H rearranged alleles[11]. However, both Pol II density and anti-sense transcripts decreased substantially within 2 kb 5′ of the DJ_H junction as compared to the peak near the DJ_H junction. We conclude that D_H recombination leads to chromatin activation and transcription that is highly restricted close to the DJ_H junction.

Since the most prominent ACE at the *Igh* locus is the intronic enhancer E_μ, we determined if the changes in the abundance of histone modifications at the DJ_H junction were dependent on E_μ by analyzing the status of DJ_H junctions in v-abl transformed pro-B cell lines from E_μ-deficient mice. We performed ChIP assays using antibodies to H3K9ac and H3K4me3 on three E_μ-deficient cell lines: FA3, which had two *Igh* alleles in the germline configuration; FA8, which had a DSP2.8-J_H3 rearrangement in one allele and a DQ52-J_H2 rearrangement in the other allele; and FA10, which had a DSP2.7-J_H2 rearranged allele and a germline allele. We used the E_μ-sufficient 6312 cell line as control for these positive modifications at the *Igh* locus. We found that in the absence of E_μ, both the germline and the DJ_H rearranged loci were completely devoid of these active histone marks, indicating that activating histone modifications associated with DJ_H junctions required the intronic enhancer E_μ (Supplementary Fig. 2).

To get an independent measure of activation, we assayed DNase I sensitivity of the DSP2.2b-J_H1 allele in 2B9 cells using a PCR assay. The E_μ-associated DNase I hypersensitive site and inactive $C_\gamma3$ sequences served as positive and negative controls, respectively. We found increased sensitivity of an amplicon 1 kb 5′ of the rearranged DSP2.2b gene segment compared to unrearranged DSP2.2b in 6312 cells (Fig. 1c). An amplicon closer to the DJ_H junction was also more DNase I sensitive in 2B9 cells than in the parental cells, although overall sensitivity at this site was not as great as at the −1 kb region, suggesting that the −1 kb region represented a weak DNase I hypersensitive site. However, increased DNase I sensitivity did not extend to upstream unrearranged DSP2 gene segments (Fig. 1c, labeled DSP2s), which were comparably insensitive in 2B9 and 6312 cells. These observations indicate that the chromatin state of a recombined D_H gene segment is selectively altered relative to unrearranged D_H gene segments on the same allele.

To further corroborate the idea that DJ_H junctions were locally activated, we examined the histone modification status of unrearranged D_H gene segments in cells that contained DJ_H recombined alleles. Unrearranged DSP2 gene segments in 2B9 cells were inactive by several criteria; they lacked H3K9ac and H3K4me3 and retained H3K9me2 (Fig. 2b, labeled DSP2s). The same was true in a different cell line, 2F1, that had undergone DQ52 to J_H1 rearrangement in one allele and DSP2.2a to J_H2 rearrangement in the second allele (Fig. 2a,c). We also interrogated sequences around DFL16.1 in these cells to determine whether D_H rearrangements affected the peak of activation at the 5′ end of the D_H-C_μ domain. We found that neither DSP2.2b nor DQ52 rearrangement affected the activation state of DFL16.1 positively or negatively (Fig. 2, amplicons labeled DFL). Consistent with this observation, DNase I sensitivity of the unrearranged DFL16.1 was not altered on DSP2.2b-rearranged alleles (Fig. 1c). We conclude that D_H recombination leads to highly localized histone modification and accessibility changes at DJ_H junctions that do not extend to germline D_H gene segments that lie upstream.

Chromatin changes at uniquely located D_H gene segments

Unlike the intervening DSP2 gene segments, the 5′-most and 3′-most D_H gene segments are associated with active chromatin marks in the germline configuration. To determine whether rearrangements of these gene segments also lead to additional local chromatin activation, we

investigated the state of a DFL16.1-J_H1 recombined allele in 2C10 cells and a DQ52-J_H1 recombined allele in 2F1 cells (Fig. 3a). The sequences upstream of DFL16.1 were lost in the second allele of 2C10 cells, which had undergone V_H to DJ_H recombination, and the sequences immediately upstream of DQ52 were lost in the second allele of 2F1 cells, which had rearranged an upstream D_H gene segment (DSP2.2a-J_H2). This configuration of rearrangements in the two cell lines allowed us to unequivocally probe the chromatin state surrounding rearranged DFL16.1 and DQ52 gene segments.

H3K9ac abundance was substantially higher close to the recombined DFL16.1-J_H1 junction compared to the same location in germline configuration (Fig. 3b). Increased H3K9ac also was evident at DFL16.1 (−1.7), the approximate position of the H3K9ac peak in the unrearranged state, but dropped off rapidly thereafter. The same trend was evident with H3K4me3 modification (Fig. 3b). We observed no major changes in H3K4me2 or H3K9me2 modifications around the rearranged DFL16.1 compared to germline DFL16.1 (Fig. 3b). The net result of these changes was that, in addition to increased abundance of activation modifications, the peak of modifications moved to the DJ_H junction rather than being located 1.7 kb 5′ of DFL16.1. DQ52 rearrangement also increased local H3K9ac and H3K4me3 modifications (Fig. 3c), however, the fold change was much less compared to DFL16.1 or DSP2 rearrangements. This result is probably because germline DQ52 already contains abundant activating histone modifications due to its proximity to the J_H region and the nearby PQ52 promoter. The restriction of activation marks close to DQ52 was most dramatically exemplified by the sharp increase in suppressive H3K9me2 modifications within 2 kb 5′ of the DJ_H junction (Fig. 3c). Even though we noted changes in the abundance of histone modifications at DJ_H junctions involving DFL16.1 and DQ52, we did not observe any changes in DNase I sensitivity at or near these junctions (Supplementary Figs. 3,4) compared to corresponding locations near the germline D_H gene segments. These observations demonstrate that chromatin alterations in response to DJ_H recombination are highly localized regardless of D_H gene usage.

We hypothesize that localized changes that distinguish DJ_H junctions from upstream unrearranged D_H gene segments provide a plausible mechanism for targeting V_H recombination to the DJ_H junction. In this regard DSP2.9 occupies a special position within the D_H cluster. As the first D_H gene segment 3′ of DFL16.1, it is closest to the pocket of active chromatin at the 5′ end of the germline D_H cluster other than DFL16.1 itself. It is therefore possible that chromatin changes associated with DSP2.9 recombination could lead to a large domain of activated chromatin that encompassed both DSP2.9 (rearranged) and DFL16.1 (unrearranged) gene segments. Alternatively, a DSP2.9 rearranged allele may contain two distinct mini-domains of active chromatin. To distinguish between these alternatives we examined the structure of a DSP2.9-J_H2 rearranged allele in 1E3 cells, which have a DFL16.1-J_H1 rearrangement in the other allele (Fig. 4a). Remarkably, we again noted highly localized increase in H3K9ac and transcription-associated H3K4me3 at the DJ_H junction, which dropped off rapidly 3.4 kb 5′ of DSP2.9 (Fig. 4b); this amplicon is located about 3.4 kb 3′ of DFL16.1. Conversely, inhibitory H3K9me2 marks were absent at the recombined junction compared to germline DSP2.9 (Fig. 4b). Though the pattern of H3K4me2 modification was less precisely restricted to the DSP2.9-J_H2 junction, overall DSP2.9 rearrangement also resulted in local enhancement of activating histone modifications at the DJ_H junction.

These epigenetic changes were accompanied by increased DNase I sensitivity of the sequences 5′ of the DJ_H junction (Fig. 4c). An amplicon 1.5 kb 5′ of the rearranged DSP2.9 was substantially more sensitive to DNase I digestion than the corresponding region around germline DSP2.9. This increased sensitivity of the rearranged allele was not apparent 3.4 kb 5′ of DSP2.9. Additionally, DNase I sensitivity of germline DFL16.1 was comparable

between DSP2.9 rearranged and unrearranged alleles. We conclude that DSP2.9 behaves exactly like other D_H gene segments analyzed in this study and DSP2.9 rearrangement does not significantly alter the chromatin state around DFL16.1.

Chromatin modifications at DJ_H junctions in primary Pro-B cells

To determine whether DJ_H rearrangement-associated chromatin changes were present in primary pro-B cells, we performed micro-ChIP on bone marrow pro-B cells isolated by flow cytometry. To account for the heterogeneity of bone marrow pro-B cells, we used a pan-DSP primer that hybridized to all 6 DSP gene segments and one that was unique to DFL16.1, together with a J_H1 primer (Fig. 5a) to assay the histone modification state of DJ_H1 junctions by real-time PCR. We found that H3K9ac as well as H3K4me3 marks were substantially higher at DFL16.1-J_H1 and DSP2-J_H1 junctions compared to the corresponding germline D_H segments (Fig. 5b). γ-actin promoter and β-globin amplicons served as positive and negative controls. To examine the chromatin state of DJ_H junctions that utilized other J_H gene segments, we used a reverse primer located 3′ of J_H4; for these assays the PCR reaction was followed by Southern blotting (Fig. 5c) and quantification of the signals from the Southern blots (Fig. 5d). We compared PCR products from 0.1–0.2 ng of ChIP material to a serial dilution of input material (2.0, 1.0 and 0.5 ng for DJ_H junctions; 0.8, 0.2 and 0.05 ng for germline fragments). In two independent H3K4me3 ChIPs and one H3K9ac ChIP we found that DJ_H junctions, but not germline D_H gene segments, were enriched in ChIP DNA compared to input DNA. Taken together, both assays demonstrate that DJ_H junctions are selectively targeted for epigenetic modifications implicated in RAG1-RAG2 recruitment.

Restricted recruitment of recombinase to DJ_H junctions

To determine whether DJ_H junction-localized changes in histone modifications correlated with recombinase recruitment, we used chromatin immunoprecipitation to locate RAG1 on DJ_H recombined alleles. We started with a pro-B cell line that lacks endogenous RAG1 and is transgenic for the catalytically inactive RAG1(D708A) mutant (D345 cells), in which the *Igh* locus is in the germline configuration[20]. We transiently expressed RAG1 in D345 cells and identified single-cell clones that had undergone D_H recombination. We used 3 such lines in our assays (Fig. 6a); clone 3E had a DSP2.2-J_H2 rearranged allele, while clones 1C6 and 2C11 had DFL16.1-J_H1 and DFL16.1-J_H4 rearrangements; the other allele in all three clones was in germline configuration.

Using a RAG1-specific antibody in ChIP, we found that RAG1 was highly enriched in the J_H region and completely depleted over most D_H gene segments in D345 cells as previously shown (Fig. 6b,c)[20]. Interestingly, we noticed a small peak of RAG1 coincident with low amounts of activating histone modifications just 5′ of DFL16.1. RAG1 density peaked approximately 1.7 kb upstream of DFL16.1, as previously noted for H3K9ac and H3K4me3 peaks[11]. This peak may represent a “spill-over” of RAG proteins from the J_H-associated recombination center because of the spatial proximity of DFL16.1 to the J_H domain[21]

We found more RAG1 at the recombined DSP2.2-J_H2 junction in 3E cells (Fig. 6b). However, RAG1 binding was close to background (represented by the β-globin amplicon) at upstream unrearranged DSP2.9 and DFL16.1 gene segments. The pattern of RAG2 recruitment in these cells was similar to that seen with RAG1 (Supplementary Fig. 5). Thus, both RAG1 and RAG2 were highly enriched at a recombined DSP2.2 gene segment. Similarly, RAG1 density was substantially higher at the recombined DFL16.1-J_H1 junction in 1C6 cells, compared to unrearranged DFL16.1 gene segment in the same cells (Fig. 6c, compare amplicon labeled DFL-J_H1 to those labeled DFL and DFL(+1.2)). The same pattern of RAG1 binding was noted in an independently derived DFL16.1 rearranged cell line

(clone 2C11, Supplementary Fig. 6). We confirmed that the histone modification pattern of the D345 derivatives closely resembled the pattern of 6312-derived clones shown in Figs. 1–3 (Supplementary Fig. 7). We conclude that D_H recombination leads to accumulation of RAG proteins at DJ_H junctions.

The high RAG1 density at DFL16.1-J_H1 in 1C6 cells indicated that the RAG1 peak centered 5′ of DFL16.1 on unrearranged alleles shifted to the DFL16.1-J_H junction after recombination (compare RAG1 at DFL16.1-J_H1 to RAG1 at DFL(−1.7) which represents both recombined and germline alleles). This result is directly analogous to the shift in histone modification peaks seen on DFL16.1-J_H1 recombined alleles (Fig. 3b). Moreover, we noted that RAG1 density was higher at DJ_H junctions compared to the germline J_H4 region in both rearranged cell lines. Because RAG protein density in the germline *Igh* locus is concentrated over the J_H gene segments, these observations suggest that RAG1 and RAG2 re-distribute towards the DJ_H junctions on rearranged alleles. We propose that re-focusing RAG1-RAG2 not only maximizes utilization of the DJ_H RSS for V_H recombination, but also serves to limit the low but detectable occurrence of direct V_H to J_H rearrangements[26]

DISCUSSION

Three regulatory features are shared by all V_H gene recombination. Firstly, V_H recombination always follows D_H recombination (timing). This timing could be mediated by a late-acting ACE associated with V_H gene segments, such that D_H recombination would have always occurred before this ACE was activated. However, such an ACE has not been identified. Secondly, V_H recombination is selectively activated on alleles that have undergone D_H recombination (allele specificity). This under-appreciated facet of V_H recombination can be inferred from the state of *Igh* alleles in core RAG knock-in mice[27,28]. A substantial number of mature B cells that develop in these strains contain one *Igh* allele in germline configuration, compared to normal B cells where both *Igh* alleles are invariably rearranged. These observations indicate that recombination is preferentially completed on DJ_H recombined alleles. Thirdly, V_H gene segments recombine precisely to the RSS associated with DJ_H junctions, while excluding virtually identical RSSs associated with germline D_H gene segments on the same allele (precision). These universal features must be accounted for in any model for activation of V_H recombination. Here we propose such a model based on our analyses of DJ_H recombined alleles.

We propose that V_H recombination follows D_H recombination because it is only after the formation of DJ_H junctions that RAG proteins have ready access to the 5′-RSS of D_H genes. Prior to initiation of recombination RAG density is primarily located over the J_H gene segments. In accordance with prevailing models of RSS synapsis and hairpin formation, an initiating RAG complex at a J_H-RSS would seek and pair with a D_H-RSS (because of 12/23 complementarity), thereby initiating D_H recombination. After D_H recombination RAG proteins are preferentially recruited to DJ_H junctions, permitting them to initiate the reaction at the 5′ D_H-RSS; now the complementary RSS would be that of a V_H gene segment, thereby leading to V_H recombination. This model extends the recombination center model for germline antigen receptor loci to DJ_H recombined alleles. Essentially, D_H recombination brings D_H-RSSs into the recombination center to permit the second step of *Igh* gene assembly. The notion that D_H RSSs become available to initiate recombination only after DJ_H recombination also provides a ready explanation for allele-specificity of V_H recombination.

Our model circumvents the need to invoke independent activation and recruitment of RAG proteins to V_H gene segments. Indeed, it is easy to imagine that RAG recruitment all along the 2.5 Mb V_H locus would substantially increase RAG-induced DNA breaks and

translocations. We hypothesize that restricting RAG presence to a discrete part of the *Igh* locus, while sequentially bringing in the right gene segments provides the correct recombination order while minimizing genomic instability. We do not suggest that RAG recruitment to the DJ_H RSS is sufficient to initiate V_H recombination. Rather, RAG proteins bound to the DJ_H-associated RSS must find and gain access to a V_H RSS in order for hairpin formation to occur. It is likely that locus conformation, mediated by looping and/or compaction, plays a role in spatially positioning V_H gene segments in the vicinity of DJ_H-associated RAG proteins. Lack of such positioning is the likely explanation for reduced distal V_H recombination in Pax5- or YY1-deficient pro-B cells[29,30]. Additionally, correctly positioned V_H gene segments must also be in the appropriate chromatin state for RAG proteins to recognize the V_H RSS and induce nicking. The permissive chromatin state required for V_H access may be conferred in part by interleukin 7-dependent histone modifications[19,31–34] and Pax5-dependent loss of H3K9me2 (ref. 12).

One caveat to the model is that DQ52-associated RSSs, that are RAG-rich prior to rearrangement, should be able to recombine with germline V_H gene segments to produce V_H-DQ52 junctions. Indeed, such rearrangements are in fact observed, but only when the spatial configuration of the *Igh* locus is altered. The first instance of V_H to germline D_H recombination was observed in mice where a V_H gene segment was “knocked in” very close to DFL16.1 (ref. 35). This V_H gene segment rearranged preferentially to DQ52 located 50 kb away, rather than to DFL16.1 located only 1.0 kb away. This product was likely generated by RAG binding at an unrearranged DQ52, followed by capture of the RSS associated with the knocked-in V_H. We propose that synapsis between germline DQ52 and the knocked-in V_H is possible in this situation because both gene segments lie within the same chromatin domain that is demarcated by CTCF and YY1 binding sites 5′ of DFL16.1 (refs. 21, 22). In the normal configuration of the *Igh* locus, RAG-bound complexes at DQ52 RSSs would be more effectively captured by J_H RSSs because V_H gene segments are located outside the D_H domain[21].

A second instance of V_H to germline DQ52 rearrangement was observed[22] on *Igh* alleles mutated at the two CTCF-binding elements upstream of DFL16.1 (ref. 23). These modifications remove the newly identified looping or barrier sites 5′ of DFL16.1 that sequester all D_H gene segments in one chromatin domain[21,22]. In the absence of the normal looping or barrier sites perhaps the D_H domain extends into the proximal V_H region, thereby incorporating one or more V_H gene segments into the D_H domain. Functionally, this would be analogous to the proposed structure generated on the allele with the knocked-in V_H gene segment described above. Therefore, V_H RSS(s) would be available for synapsis with the DQ52 RSS leading to proximal V_H to germline DQ52 rearrangements.

Finally, our observations provide a plausible mechanism for the precision of V_H recombination to DJ_H junctions but not to germline D_H-RSSs that lie 4 kb upstream. Specifically, we found that activating histone modifications and nuclease sensitivity of DJ_H junctions did not extend even 4 kb to the closest unrearranged D_H gene segment. Because these changes occur in recombinase-deficient cells, our working hypothesis is that these changes direct RAG recruitment to DJ_H junctions while avoiding germline D_H gene segments that lie 5′. Consistent with this idea, direct analysis of RAG binding also showed highest amounts of RAG1-RAG2 at DJ_H junctions and very little at germline D_H gene segments. Interestingly, RAG density appeared to shift from its pre-rearrangement position over J_H gene segments to focused accumulation at DJ_H junctions, thereby further accentuating the use of the DJ_H-RSS in the next recombination step. We propose that the exquisite specificity of V_H recombination to DJ_H junctions is imposed by the localized changes in chromatin structure and consequent restriction of RAG proteins to DJ_H junctions.

Several mechanisms can be considered by which chromatin changes are restricted to DJ_H junctions. First, since large portions of the D_H region are actively maintained in silent (H3K9me2-marked) chromatin[11], it is possible that some of these heterochromatin-associated enzymes are brought along with the recombining D_H gene segment. After rearrangement though, the D_H promoter is activated by proximity to E_μ and results in activation/transcription-associated histone modifications close to the DJ_H junction. However, these modifications cannot spread 5′ due to silencing activities located there. Secondly, D_H promoters activate bi-directional transcription after rearrangement[11]. It is possible that elevated levels of antisense transcripts that are generated from the D_H promoter may play a role in maintaining the heterochromatic state of upstream germline D_H gene segments. Third, D_H promoters may function as boundary elements. In this scenario, though the D_H gene segment recombines into the highly active J_H region, the positive effect of this part of the locus is prevented from spreading into the upstream germline D_H gene segments by the newly active rearranged D_H promoter. Further studies are needed to determine the factors that restrict chromatin structural changes to DJ_H junctions.

METHODS

Cell Culture

Rag2$^{-/-}$ 6312 cells and its derivative cell lines 2B9, 2C10, 2F1 and 1E3 as well as Bcl2-Tg RAG1 D708A-Tg/D345 cells and its derivatives 3E, 1C6 and 2C11 were grown in RPMI media supplemented with fetal bovine serum, antibiotics and 2-mercaptoethanol. The DJ_H-rearranged derivative cells were generated by transient transfection of a RAG2 expression vector into 6312 cells or a RAG1 expression vector into D345 cells, followed by single cell cloning and characterization of DJ_H junctions by PCR. Briefly, a bicistronic retroviral vector that coexpressed RAG2 and GFP was transfected into 6312 cells or retroviral vectors expressing RAG1 and RFP were co-transfected into D345 cells using Amaxa nucleofector (Cell Line Nucleofector Kit V, Program W-01). 24 h after transfection, GFP-positive 6312 cells and RFP-positive D345 cells were sorted and grown in RPMI culture medium. After 4 to 7 days of culture, GFP-negative 6312 and RFP-negative D345 cells were single-cell sorted into 96-well dishes for expansion. Clones were screened for the presence of DJ_H recombined alleles by PCR and chosen to represent a range of D_H segment usage. Generation of the v-Abl transformed 6312 and D345 cells has been described previously[20,36].

Chromatin Immunoprecipitaion (ChIP)

ChIPs for modified histones and RAG1 were performed as previously described[11,20]. Antibodies for ChIP were purchased from the following sources: H3K9ac (06–942) and H3K9me2 (07–441) from Millipore; H3K4me2 (39141) and H3K4me3 (39159) from Active Motif. Hybridoma cell lines producing monoclonal antibodies for RAG1 (#23) or RAG2 (#11) were generated by Epitomics, Inc (Supplementary Fig. 8). Rabbits were immunized with either strep-RAG1 core (murine RAG1 amino acids 377–1008 fused to strep-tagII[37]) or murine RAG2 amino acids 1–490 fused to a hexahistidine tag. Hybridoma supernatants were screened against MBP-RAG1 core (murine RAG1 amino acids 384–1008 fused to maltose binding protein at the N-terminus and a hexahistidine tag at the C-terminus[38]) or murine RAG2 amino acids 1–490 fused to maltose binding protein. All RAG proteins were purified from bacteria. Input DNA and the immunoprecipitated DNA were quantified fluorometrically using PicoGreen (Molecular Probes/Life Technologies). 200–400 pg of DNA was used in each real-time PCR reaction performed in duplicates and each ChIP was performed in duplicate or triplicate. The relative abundance of specific sequences in the immunoprecipitate relative to input was analyzed as described[11] by real-time PCR using the

primers listed in Supplementary Table 1. The abundance ($IP/Input_{corr}$) of RAG1 at specific genomic loci was calculated as described before[20].

DNase I sensitivity

DNase I sensitivity assays were performed as previously described[18]. Briefly, nuclei from 2×10^6 cells were treated with increasing amounts of DNase I (0 to 2 units) followed by purification of the genomic DNA. Real-time PCR assay for each treated sample was performed in duplicate using primers listed in Supplementary Table 1. Sensitivity was determined using two independent DNase I-treated samples for each cell line.

Micro-ChIP from primary pro-B cells

Bone marrow from 16 C57BL/6 mice was labeled with biotinylated antibodies for Mac-1 (553309), Gr-1 (553125), Ter119 (553672), CD3ε (553060), IgM (553406), Ly-6C (557359) and DX-5 (553856) purchased from BD Biosciences. The labeled cells were then bound to streptavidin microbeads (130-048-102) and depleted by passing through LD columns (130-042-901), both from Miltenyi Biotec. The flow through fraction was then stained with B220-FITC, CD19-PE-Cy7, CD43-PE (553088, 552854 and 553271 respectively from BD Biosciences) and AA4.1-APC (17-5892, eBioscience) and cells expressing all four markers were sorted on a BD FACSAria cell sorter. The total yield of 1.3×10^6 pro-B cells was divided into 5 tubes, one of which was used as input material while the other four tubes were used to perform micro-ChIP in duplicate using antibodies against histone H3K9ac and H3K4me3. The micro-ChIP protocol described by Dahl and Collas was adopted with minor modifications[39]. 100 to 200 pg of ChIP samples was analyzed by real-time PCR (Fig. 5a) or by Southern blot of PCR products (Fig. 5b) to determine the enrichment of specific targets. For Southern blots, we performed one round of PCR of 35 cycles (for DJ_H rearrangement analysis) or of 32 cycles (for germline fragments). The sequence of primers and probes used in the assay are listed in Supplementary Table 1. Animal experiments were reviewed and approved by the NIA/IRP Animal Care and Use Committee (Animal Studies Protocol # 338-LMBI-2013)

Statistical analysis

The average values and standard deviations for all ChIP experiments as well as DNase I sensitivity assays were calculated in Microsoft Office Excel 2007. Graphs were generated in either GraphPad Prism 5 or Microsoft Office Excel 2007.

Supplementary Material

Refer to Web version on PubMed Central for supplementary material.

Acknowledgments

This research was supported by the Intramural Research Program of the National Institute on Aging, Baltimore, MD, and by NIH grants to F.W.A. (AI20047) and D.G.S. (AI32524). F.W.A. and D.G.S. are Investigators of the Howard Hughes Medical Institute.

REFERENCES

1. Bergman Y, Cedar H. Epigenetic control of recombination in the immune system. Semin Immunol. 2010; 22:323–329. [PubMed: 20832333]
2. Schatz DG, Ji Y. Recombination centres and the orchestration of V(D)J recombination. Nat Rev Immunol. 2011; 11:251–263. [PubMed: 21394103]
3. Perlot T, Alt FW. Cis-regulatory elements and epigenetic changes control genomic rearrangements of the IgH locus. Adv Immunol. 2008; 99:1–32. [PubMed: 19117530]

4. Thomas LR, Cobb RM, Oltz EM. Dynamic regulation of antigen receptor gene assembly. Adv Exp Med Biol. 2009; 650:103–115. [PubMed: 19731805]
5. Blackwell TK, et al. Recombination between immunoglobulin variable region gene segments is enhanced by transcription. Nature. 1986; 324:585–589. [PubMed: 3491327]
6. Yancopoulos GD, Alt FW. Developmentally controlled and tissue-specific expression of unrearranged VH gene segments. Cell. 1985; 40:271–281. [PubMed: 2578321]
7. Osipovich O, Oltz EM. Regulation of antigen receptor gene assembly by genetic-epigenetic crosstalk. Semin Immunol. 2010; 22:313–322. [PubMed: 20829065]
8. Spicuglia S, Pekowska A, Zacarias-Cabeza J, Ferrier P. Epigenetic control of Tcrb gene rearrangement. Semin Immunol. 2010; 22:330–336. [PubMed: 20829066]
9. Subrahmanyam R, Sen R. Epigenetic Features that Regulate IgH Locus Recombination and Expression. Curr Top Microbiol Immunol. 2011; 356:39–63. [PubMed: 21779986]
10. Subrahmanyam R, Sen R. RAGs' eye view of the immunoglobulin heavy chain gene locus. Semin Immunol. 2010; 22:337–345. [PubMed: 20864355]
11. Chakraborty T, et al. Repeat organization and epigenetic regulation of the DHCmu domain of the immunoglobulin heavy-chain gene locus. Mol Cell. 2007; 27:842–850. [PubMed: 17803947]
12. Johnson K, et al. B cell-specific loss of histone 3 lysine 9 methylation in the V(H) locus depends on Pax5. Nat Immunol. 2004; 5:853–861. [PubMed: 15258579]
13. Osipovich O, et al. Targeted inhibition of V(D)J recombination by a histone methyltransferase. Nat Immunol. 2004; 5:309–316. [PubMed: 14985714]
14. Liu Y, Subrahmanyam R, Chakraborty T, Sen R, Desiderio S. A plant homeodomain in RAG-2 that binds Hypermethylated lysine 4 of histone H3 is necessary for efficient antigen-receptor-gene rearrangement. Immunity. 2007; 27:561–571. [PubMed: 17936034]
15. Matthews AG, et al. RAG2 PHD finger couples histone H3 lysine 4 trimethylation with V(D)J recombination. Nature. 2007; 450:1106–1110. [PubMed: 18033247]
16. Ramon-Maiques S, et al. The plant homeodomain finger of RAG2 recognizes histone H3 methylated at both lysine-4 and arginine-2. Proc Natl Acad Sci U S A. 2007; 104:18993–18998. [PubMed: 18025461]
17. Johnston CM, Wood AL, Bolland DJ, Corcoran AE. Complete sequence assembly and characterization of the C57BL/6 mouse Ig heavy chain V region. J Immunol. 2006; 176:4221–4234. [PubMed: 16547259]
18. Chakraborty T, et al. A 220-nucleotide deletion of the intronic enhancer reveals an epigenetic hierarchy in immunoglobulin heavy chain locus activation. J Exp Med. 2009; 206:1019–1027. [PubMed: 19414554]
19. Chowdhury D, Sen R. Stepwise activation of the immunoglobulin mu heavy chain gene locus. EMBO J. 2001; 20:6394–6403. [PubMed: 11707410]
20. Ji Y, et al. The in vivo pattern of binding of RAG1 and RAG2 to antigen receptor loci. Cell. 2010; 141:419–431. [PubMed: 20398922]
21. Guo C, et al. Two forms of loops generate the chromatin conformation of the immunoglobulin heavy-chain gene locus. Cell. 2011; 147:332–343. [PubMed: 21982154]
22. Guo C, et al. CTCF-binding elements mediate control of V(D)J recombination. Nature. 2011; 477:424–430. [PubMed: 21909113]
23. Featherstone K, Wood AL, Bowen AJ, Corcoran AE. The mouse immunoglobulin heavy chain V-D intergenic sequence contains insulators that may regulate ordered V(D)J recombination. J Biol Chem. 2010; 285:9327–9338. [PubMed: 20100833]
24. Degner-Leisso SC, Feeney AJ. Epigenetic and 3-dimensional regulation of V(D)J rearrangement of immunoglobulin genes. Semin Immunol. 2010; 22:346–352. [PubMed: 20833065]
25. Hewitt SL, Chaumeil J, Skok JA. Chromosome dynamics and the regulation of V(D)J recombination. Immunol Rev. 2010; 237:43–54. [PubMed: 20727028]
26. Koralov SB, Novobrantseva TI, Hochedlinger K, Jaenisch R, Rajewsky K. Direct in vivo VH to JH rearrangement violating the 12/23 rule. J Exp Med. 2005; 201:341–348. [PubMed: 15699070]
27. Akamatsu Y, et al. Deletion of the RAG2 C terminus leads to impaired lymphoid development in mice. Proc Natl Acad Sci U S A. 2003; 100:1209–1214. [PubMed: 12531919]

28. Dudley DD, et al. Impaired V(D)J recombination and lymphocyte development in core RAG1-expressing mice. J Exp Med. 2003; 198:1439–1450. [PubMed: 14581608]
29. Hesslein DG, et al. Pax5 is required for recombination of transcribed, acetylated, 5' IgH V gene segments. Genes Dev. 2003; 17:37–42. [PubMed: 12514097]
30. Liu H, et al. Yin Yang 1 is a critical regulator of B-cell development. Genes Dev. 2007; 21:1179–1189. [PubMed: 17504937]
31. Bertolino E, et al. Regulation of interleukin 7-dependent immunoglobulin heavy-chain variable gene rearrangements by transcription factor STAT5. Nat Immunol. 2005; 6:836–843. [PubMed: 16025120]
32. Chowdhury D, Sen R. Transient IL-7/IL-7R signaling provides a mechanism for feedback inhibition of immunoglobulin heavy chain gene rearrangements. Immunity. 2003; 18:229–241. [PubMed: 12594950]
33. Stanton ML, Brodeur PH. Stat5 mediates the IL-7-induced accessibility of a representative D-Distal VH gene. J Immunol. 2005; 174:3164–3168. [PubMed: 15749844]
34. Xu CR, Schaffer L, Head SR, Feeney AJ. Reciprocal patterns of methylation of H3K36 and H3K27 on proximal vs. distal IgVH genes are modulated by IL-7 and Pax5. Proc Natl Acad Sci U S A. 2008; 105:8685–8690. [PubMed: 18562282]
35. Bates JG, Cado D, Nolla H, Schlissel MS. Chromosomal position of a VH gene segment determines its activation and inactivation as a substrate for V(D)J recombination. J Exp Med. 2007; 204:3247–3256. [PubMed: 18056289]
36. Shinkai Y, et al. RAG-2-deficient mice lack mature lymphocytes owing to inability to initiate V(D)J rearrangement. Cell. 1992; 68:855–867. [PubMed: 1547487]
37. Ciubotaru M, et al. RAG1-DNA binding in V(D)J recombination. Specificity and DNA-induced conformational changes revealed by fluorescence and CD spectroscopy. J Biol Chem. 2003; 278:5584–5596. [PubMed: 12488446]
38. Fugmann SD, Villey IJ, Ptaszek LM, Schatz DG. Identification of two catalytic residues in RAG1 that define a single active site within the RAG1/RAG2 protein complex. Mol Cell. 2000; 5:97–107. [PubMed: 10678172]
39. Dahl JA, Collas P. A rapid micro chromatin immunoprecipitation assay (microChIP). Nat Protoc. 2008; 3:1032–1045. [PubMed: 18536650]

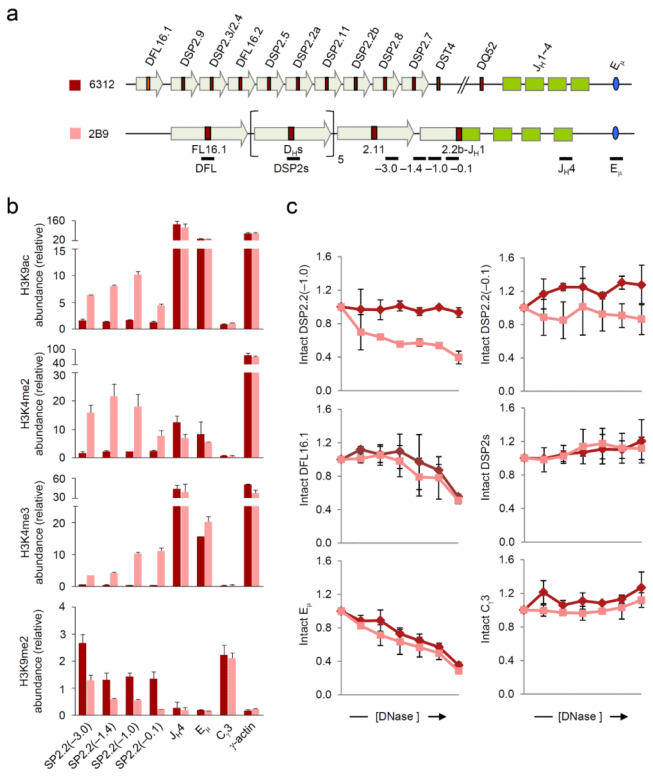

Figure 1. Chromatin accessibility at DSP2.2b-J_H1 rearranged allele

(**a**) Schematic of the germline *Igh* locus in 6312 cells and the DJ_H rearranged *Igh* locus in 6312-derivative 2B9 cells, which harbor a DSP2.2b-J_H1 junction in one allele and a V_H rearrangement in the other allele (not to scale). The positions of amplicons analyzed by real-time PCR are also shown. Block arrows represent D_H-associated repeat sequences[10,11]. (**b**) ChIP assays were performed using antibodies for modified histones as indicated with chromatin obtained from 6312 (maroon bars) and 2B9 (pink bars) cells. The numbers within the parentheses indicate positions in kb 5′ of the DSP2.2b segment. All samples were assayed in duplicate by real-time PCR and relative abundance (*y* axis) for each amplicon in the immunoprecipitate was calculated as previously described[11]. γ-actin promoter and $C_\gamma3$ served as controls for active and inactive chromatin, respectively. Data show the average of 2 independent ChIP experiments and error bars indicate standard deviation. (**c**) DNase I sensitivity analyses of the DSP2.2b-J_H1 allele (pink lines) compared to the germline *Igh* allele (maroon lines). 2×10^6 nuclei from 6312 and 2B9 cells were treated with increasing concentrations of DNase I (*x* axis, 0 to 2 units of DNase I) followed by purification of the genomic DNA. All samples were assayed in duplicate by quantitative real-time PCR and the proportion of intact DNA (*y* axis) at each DNase I concentration was determined for the indicated amplicon as previously described[18]. E_μ corresponds to the known DNase I hypersensitive site in the J_H-C_μ intron, while $C_\gamma3$ is DNase I insensitive. Data show the average of 2 independent DNase I sensitivity experiments and error bars indicate standard deviation.

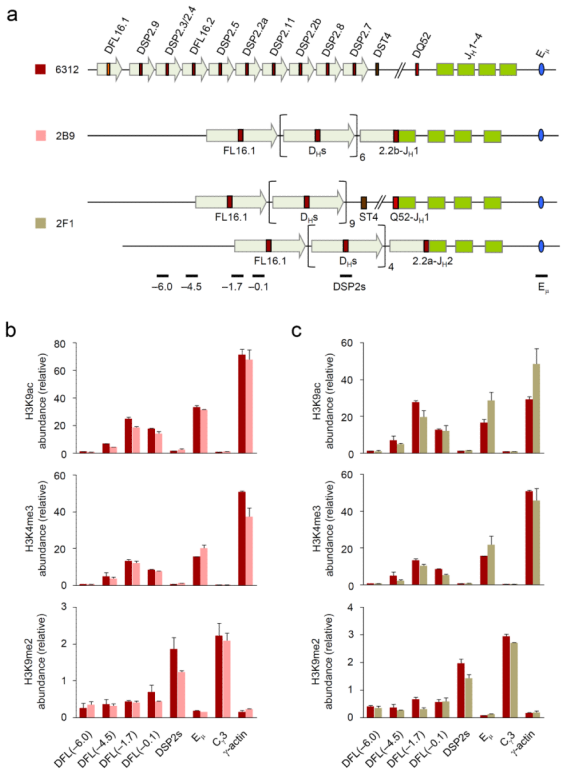

Figure 2. Histone modifications at unrearranged upstream D_H gene segments in DJ_H rearranged *Igh* alleles

(**a**) Schematic of the germline *Igh* locus in 6312 cells and the rearranged loci in the 6312-derivatives 2B9 and 2F1 cells are shown (not to scale). 2B9 cells have a DSP2.2b-J_H1 rearrangement on one allele and a V_H rearrangement on the second allele; 2F1 cells have DQ52-J_H1 and DSP2.2a-J_H2 rearrangements. These configurations leave 7 germline D_H gene segments in 2B9 cells (1xDFL16.1, 1xDFL16.2 and 5xDSP2); 2F1 cells have 10 germline D_H gene segments (1xDFL16.1, 1xDFL16.2 and 8xDSP2) in the DQ52-J_H1 rearranged allele and 5 germline D_H gene segments (1xDFL16.1, 1xDFL16.2 and 3xDSP2) in the DSP2.2a-J_H2 rearranged allele. The positions of amplicons analyzed by real-time PCR are also shown. (**b**, **c**) ChIP assay was performed using antibodies for modified histones as indicated with chromatin obtained from 6312 (maroon bars), 2B9 (**b**, pink bars) and 2F1 (**c**, light green bars) cells. Real-time PCR assays were performed in duplicate for the indicated amplicons to determine the chromatin status of upstream unrearranged D_H gene segments that remain on DJ_H rearranged alleles. Numbers within parentheses indicate the position of amplicons in kb 5′ of DFL16.1. Data show the average of 2 independent ChIP experiments and error bars indicate standard deviation.

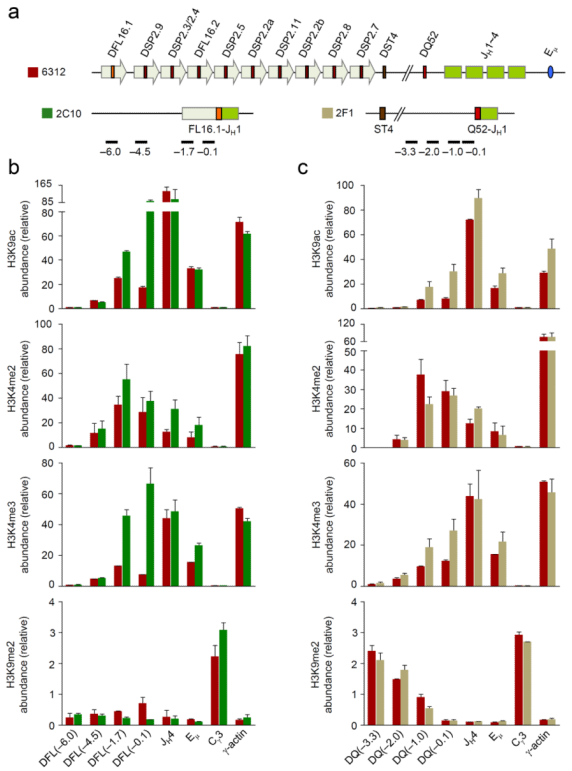

Figure 3. Histone modifications at DFL16.1- and DQ52-rearranged *Igh* alleles

(**a**) Schematic of the germline *Igh* locus in 6312 cells and the DJ_H-rearranged loci in 6312-derived 2C10 and 2F1 cells are shown (not to scale) along with the positions of amplicons analyzed by real-time PCR; 2C10 cells have a DFL16.1-J_H1 rearrangement in one allele and a V_H rearrangement in the second allele which does not score for the DFL16.1 specific primers used in part **b**). 2F1 cells have a DQ52-J_H1 rearrangement in one allele and a DSP2.2a-J_H2 rearrangement in the second allele which does not score with the DQ52-specific primers used in part **c**). (**b**, **c**) ChIP assays were performed using antibodies for modified histones as indicated, with chromatin obtained from 6312 cells (maroon bars) and derivative cell lines 2C10 (**b**, green bars) and 2F1 (**c**, light green bars). Numbers within parentheses indicate positions in kb 5′ of the rearranged D_H gene segment. Real-time PCR assays were performed in duplicate for the indicated amplicons and data show the average of 2 independent ChIP experiments with error bars indicating standard deviation.

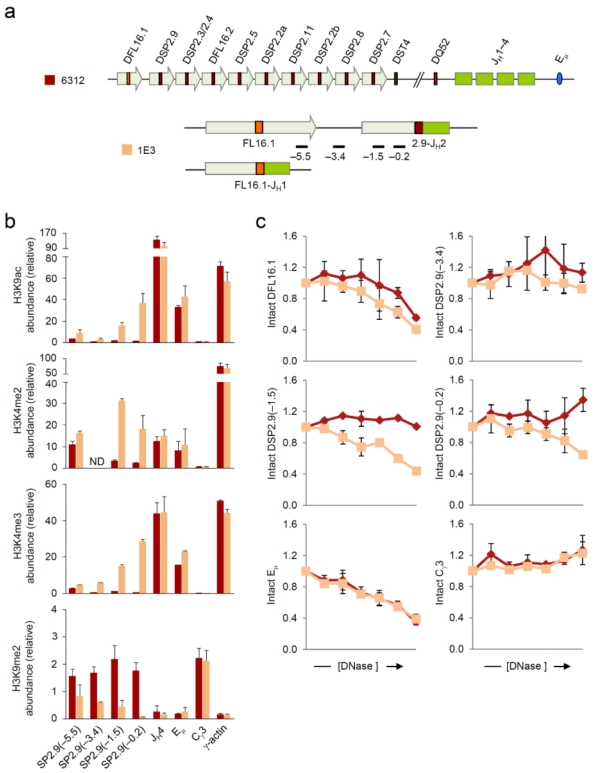

Figure 4. Chromatin accessibility at DSP2.9-J_H2 rearranged allele

(**a**) Schematic of the germline *Igh* locus in 6312 cells and the DJ_H-rearranged loci in 1E3 cells are shown (not to scale) along with the positions of amplicons analyzed by real-time PCR. 1E3 cells have a DSP2.9-J_H2 junction in one allele and a DFL16.1-J_H1 junction in the second allele which would not score for the DSP2.9-specific primers used in this assay. (**b**) ChIP assays were performed using antibodies for modified histones as indicated, with chromatin from 6312 (maroon bars) and 1E3 (orange bars) cells. Numbers within parentheses indicate positions in kb 5′ of the DSP2.9 segment. Real-time PCR assays were performed in duplicate for the indicated amplicons. Data show the average of 2 independent ChIP experiments and error bars indicate standard deviation. ND stands for `not determined'. (**c**) DNase I sensitivity analyses of the DSP2.9-J_H2 allele (orange lines) compared to the germline *Igh* allele (maroon lines). 2×10^6 nuclei from 6312 and 1E3 cells were treated with increasing concentrations of DNase I (*x* axis, 0 to 2 units of DNase I) followed by purification of the genomic DNA. All samples were assayed in duplicate by quantitative real-time PCR assay and the proportion of intact DNA (*y* axis) at each DNase I concentration was determined for the indicated amplicon as previously described[18]. E_μ corresponds to the known DNase I hypersensitive site in the J_H-C_μ intron, while $C_\gamma3$ is DNase I insensitive. Data show the average of 2 independent DNase I sensitivity experiments; error bars indicate standard deviation.

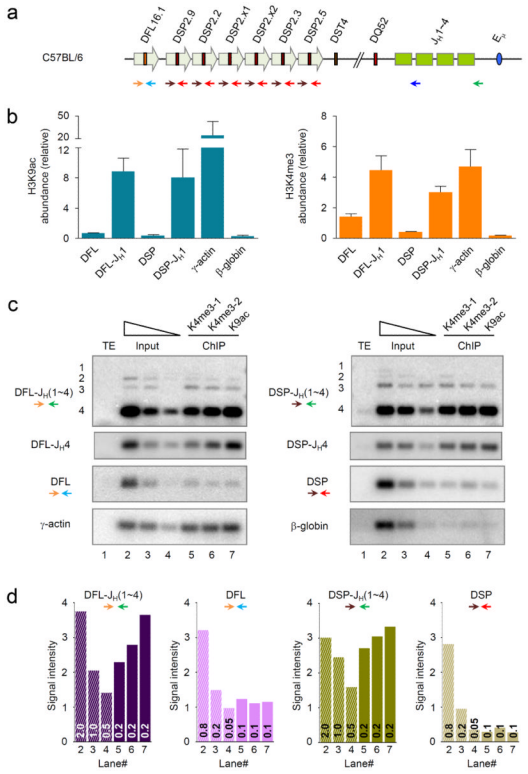

Figure 5. Chromatin accessibility at DJ_H junctions in primary pro-B cells

(**a**) Schematic of the C57BL/6 *Igh* locus and the location of primers (colored arrows) used for PCR are shown. (**b**, **c**) Micro-ChIP assays were performed with 2−2.5×10^5 pro-B cells isolated by flow cytometry from the bone marrow of C57BL/6 mice using antibodies specific for modified histones as indicated. We assayed the ChIP samples by real-time PCR (**b**) or by Southern blot of indicated PCR products (**c**). (**b**) DJ_H1 junctions were scored with forward primers that annealed 5′ of either the DFL16.1 segment (orange) or all the DSP2 segments (brown) and a reverse primer that annealed 3′ of J_H1 (blue; amplicons labeled DFL-J_H1 and DSP-J_H1). Germline DFL16.1 and DSP2 segments were assayed using the same forward primers and a reverse primer that annealed 3′ of either DFL16.1 (light blue) or all the DSP2 (red) gene segments respectively (amplicons labeled DFL and DSP). γ-actin promoter and β-globin locus served as positive and negative controls respectively for the ChIP assay. *y* axis shows the relative abundance of amplicons in the ChIP material compared to the same quantity of DNA from input material. Data show the average of 2 independent ChIP experiments using each antibody from a single isolation of bone marrow pro-B cells; error bars indicate standard deviation. (**c**) PCR amplification was carried out on micro-ChIP samples using the same D_H region forward primers and a reverse primer that annealed 3′ of J_H4 (green). Following amplification the products were fractionated by agarose gel electrophoresis, transferred to nylon membranes which were probed with radioactively labeled oligonucleotides listed in Supplementary Table 1. Serially diluted input DNA (lanes 2–4; 2, 1 and 0.5 ng for top two panels in each column; 800, 200 and 50 pg for bottom two panels in each column) was compared to either 200 pg (DJ_H junctions) or 100 pg (germline D_H, γ-actin and β-globin) of ChIP DNA from two independent H3K4me3 (lanes 5 and 6) and one anti-H3K9ac (lane 7) ChIPs. γ-actin promoter and β-globin locus served as positive and negative controls, respectively, for the ChIP assay (bottom panels). A lower exposure of the Southern blot is shown for the DJ_H4 PCR products (second panel from top in each column) since signal from these bands was saturated with the exposure

time of the top panel. (**d**) Quantitation of cumulative signal intensity of the PCR products from each lane of the Southern blots for DJ_H junctions and germline D_H gene segments shown in (**c**). The amount of template DNA (in ng) used in the PCR reactions is shown at the base of the bars; lanes 2–4 correspond to a serial dilution of input DNA and lanes 5–7 correspond to ChIP DNA from two H3K4me3 and one H3K9ac ChIPs. Data represent 3 independent PCR assays and Southern blots using different quantities of template DNA.

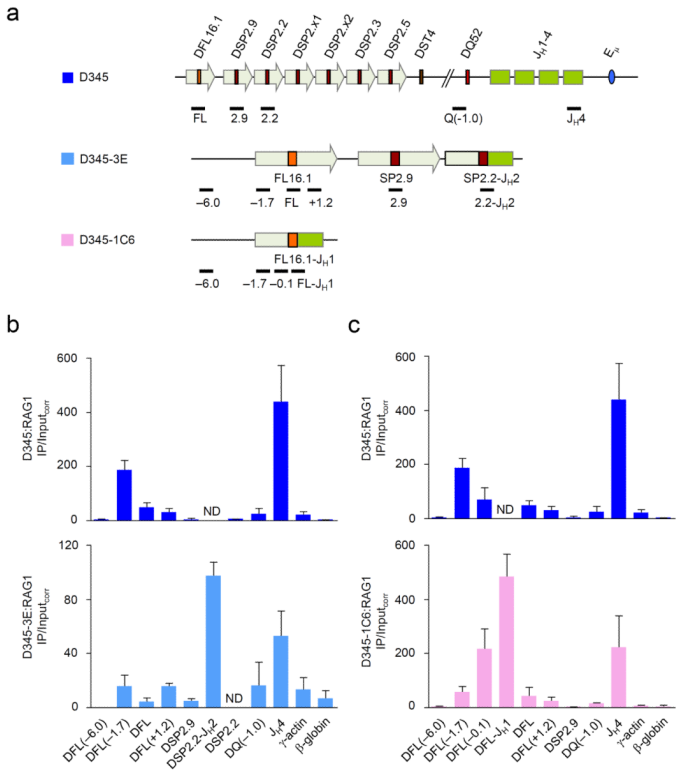

Figure 6. RAG1 association with DJ_H rearranged *Igh* alleles

(**a**) Schematic of the germline *Igh* locus in Bcl2-Tg RAG1/D708A-Tg (D345) pro-B cells[20] and the DJ_H junctions in the D345-derivatives 3E and 1C6 cells are shown (not to scale) along with the positions of amplicons analyzed by real-time PCR. 3E cells have a DSP2.2-J_H2 junction and 1C6 cells have a DFL16.1-J_H1 junction. The second allele in these cells is in germline configuration. (**b**, **c**) ChIP assays were performed with a RAG1-specific antibody in D345 (dark blue bars), 3E (**b**; light blue bars) and 1C6 (**c**; pink bars) cells. The numbers within the parentheses indicate positions in kb 5′ (−) or 3′ (+) of the indicated gene segment. Amplicons for J_H4 and β-globin served as positive and negative controls for RAG1 binding. All amplicons were assayed in duplicate by quantitative real-time PCR and IP/$Input_{corr}$ was calculated as before[20]. Data show the average of 2 or 3 independent ChIP experiments; error bars represent standard deviation between experiments. ND stands for `not determined'.